



Article

Comparison of Glyphosate-Degradation Ability of Aldo-Keto Reductase (AKR4) Proteins in Maize, Soybean and Rice

Ronghua Chen, Siwei Wang, Yue Sun , Haiqing Li, Shuqing Wan, Fei Lin * and Hanhong Xu *

State Key Laboratory for Conservation and Utilization of Subtropical Agro-Bioresources/Key Laboratory of Natural Pesticide and Chemical Biology, Ministry of Education, South China Agricultural University, Guangzhou 510642, China

* Correspondence: resistanc@scau.edu.cn (F.L.); hhxu@scau.edu.cn (H.X.); Tel.: +86-20-85285127 (H.X.)

Abstract: Genes that participate in the degradation or isolation of glyphosate in plants are promising, for they endow crops with herbicide tolerance with a low glyphosate residue. Recently, the aldo-keto reductase (AKR4) gene in *Echinochloa colona* (*EcAKR4*) was identified as a naturally evolved glyphosate-metabolism enzyme. Here, we compared the glyphosate-degradation ability of the AKR4 proteins from maize, soybean and rice, which belong to a clade containing *EcAKR4* in the phylogenetic tree, by incubation of glyphosate with AKR proteins both in vivo and in vitro. The results indicated that, except for *OsALR1*, the other proteins were characterized as glyphosate-metabolism enzymes, with *ZmAKR4* ranked the highest activity, and *OsAKR4-1* and *OsAKR4-2* exhibiting the highest activity among the AKR4 family in rice. Moreover, *OsAKR4-1* was confirmed to endow glyphosate-tolerance at the plant level. Our study provides information on the mechanism underlying the glyphosate-degradation ability of AKR proteins in crops, which enables the development of glyphosate-resistant crops with a low glyphosate residue, mediated by AKRs.

Keywords: glyphosate; aldo-keto reductase; glyphosate degradation; glyphosate-tolerant crops



Citation: Chen, R.; Wang, S.; Sun, Y.; Li, H.; Wan, S.; Lin, F.; Xu, H. Comparison of Glyphosate-Degradation Ability of Aldo-Keto Reductase (AKR4) Proteins in Maize, Soybean and Rice. *Int. J. Mol. Sci.* **2023**, *24*, 3421. <https://doi.org/10.3390/ijms24043421>

Academic Editor: Fazhan Qiu

Received: 20 January 2023

Revised: 5 February 2023

Accepted: 7 February 2023

Published: 8 February 2023



Copyright: © 2023 by the authors. Licensee MDPI, Basel, Switzerland. This article is an open access article distributed under the terms and conditions of the Creative Commons Attribution (CC BY) license (<https://creativecommons.org/licenses/by/4.0/>).

1. Introduction

Glyphosate is commonly used as a herbicide, owing to its advantages, including its high efficiency, low toxicity, and broad efficacy spectrum [1]. It mainly acts by competitively inhibiting 5-enolpyruvylshikimate-3-phosphate synthase (EPSPS) in the shikimate synthesis pathway, and sequentially disrupting the synthesis of plant-growth-regulating substances, such as aromatic amino acids, flavonoids and proteins, thereby leading to plant death [2,3]. Given its non-selective and deleterious effects, the use of glyphosate on many crops is limited. Thus, glyphosate-resistant crops are of great value as they would contribute the convenience of weeding and reduce the costs of rice production. Cope with glyphosate resistance has been generated via EPSPS-gene modification and applied in the field, leading to effective and safe weed management in modern agriculture [4,5].

Targeted and non-targeted resistance are two major ways to endow crops with resistance to a specific herbicide. EPSPS mutation or overexpression of variants can lead to a glyphosate-resistant phenotype in crops, and had been widely used in modern agriculture. Non-targeted resistance can be achieved by reducing the accumulated level of glyphosate in plants, such as by converting glyphosate to a low-toxicity substance or blocking its transport into its target [6–9]. Although EPSPS-based glyphosate resistance has been applied for many years, a concern regarding the residue of the herbicide after treatment remains [10]. Therefore, research interest is increasing in genes that participate in degradation or isolation of glyphosate in plants. Studies on glyphosate degradation at first mainly focus on microbes in the soil which have been contaminated by glyphosate. As early as 1992, it was identified that the glyphosate oxidoreductase (GOX) gene from a bacterium degrades glyphosate to aminomethyl phosphonic acid (AMPA) [11]. The *GOX* gene then transformed, along with

CP4 (a glyphosate-resistant EPSPS gene), into wheat and rape to obtain plants with high glyphosate resistance, as more glyphosate is metabolized to AMPA rapidly in transgenic lines [12,13]. Other glyphosate-metabolic genes were discovered that they encode glycine oxidase (GO) or D-amino acid oxidase (DAAO) participating in metabolizing glyphosate to yield AMPA and glyoxylate [14,15], thus endowing glyphosate resistance at the plant level [16,17]. However, to date, reports on native glyphosate-metabolizing enzymes in plants are still scarce. Several leguminous species may contain a GOX-like enzyme, but the mechanism of action is still unclear in plants [18–20]. Recently, plant endogenous enzymes that can detoxify glyphosate have emerged, all of which fall into the aldo-keto reductase (AKR) family [21,22].

The AKR superfamily is widespread in a variety of organisms, and encompasses 190 annotated proteins divided into 16 families by sequence identity [23,24]. Each AKR enzyme has three large loops on the surface of the α/β -barrel; moreover, owing to their high flexibility and low conservation, AKR enzymes have broad substrate specificity, ranging from the glucose, glucocorticoids and small carbonyl compounds to glutathione conjugates and phospholipid aldehydes, et al. [25,26]. For instance, AKR1D family members catalyze the Δ^4 -3-ketosteroids double-bond reduction to form 5β -dihydrosteroids [27–29]. AKR4C family members (AKR4C8, AKR4C9, AKR4C10 and AKR4C11) from *Arabidopsis thaliana* are involved in the detoxification of sugar-derived reactive carbonyls, and affect photosynthesis [30], as AKR4C7 from *Zea mays* induces the conversion of sorbitol to glucose [31]. The relationship between herbicide tolerance and AKRs is as follows: overexpression of *OsAKR4-1* in tobacco decreases the generation of toxic aldehydes generated by methyl viologen (paraquat) and recovers plant growth [32]. The transformation of butachlor to dicarboxylic acid and phenol was observed in *Escherichia coli* expressing AKR17A1 from *Anabaena* sp. [33,34]. In addition, the positive roles of PsAKR1, *OsAKR4-1* and EcAKR4 in glyphosate degradation have been observed [21,22,35]. However, systematic studies in AKRs of plants that are regularly exposed to glyphosate are limited.

In this study, we performed bioinformatics analysis on genes with high homology with EcAKR4. The roles of these genes in glyphosate degradation were tested in *E. coli* cells, as well as in purified proteins. *OsAKR*-overexpressing rice lines were also constructed and subjected to glyphosate treatment to show their herbicide tolerance. The findings of our study pave the way to the AKR-based development of herbicide-resistant crops with low glyphosate residue.

2. Results and Discussion

2.1. Phylogenetic Analysis of AKR in Plants

It has been demonstrated that the EcAKR4 (EcAKR4C10) gene in *Echinochloa colona* confers glyphosate resistance to plants by encoding an enzyme that metabolizes glyphosate [22]. To investigate whether AKR genes in other plants also have similar functions, homologous genes in 21 crops were selected for phylogenetic-tree construction and evolutionary relationship analysis (Table S1). Nearest-neighbour analysis showed that the 21 AKR genes formed two distinct classes. Four genes from the Monocotyledoneae species, namely *OsAKR4-1*, *TaAKR4*, *ZmAKR4*, and EcAKR4 belong to one clade, whereas the other 17 genes from the Dicotyledoneae species were grouped in one clade (Figure 1A). This result indicated that the AKR4 genes underwent differentiation after the evolution of Monocotyledoneae and Dicotyledoneae [36].

The conserved domain of functional EcAKR4 with Pfam (PF00248) was applied to identify homologs of AKRs in rice by using SMART and NCBI CDD. A total of 29 AKR genes were identified in the rice whole genome. According to the results of phylogenetic-tree analysis, they were grouped into five subfamily clades, namely Groups 1 to 5. The *OsAKR4-1* genes were clustered in Group 4 with another five genes, and they were designated as *OsAKR4-2* (Os01g62870), *OsAKR4-3* (Os01g62880), *OsAKR4-4* (Os02g03100), *OsALR1* (Os05g38230), and *OsALR2* (Os05g39690), with 89%, 68%, 41%, 71%, and 46% amino-acid identity to *OsAKR4-1*, respectively (Figure 1B).

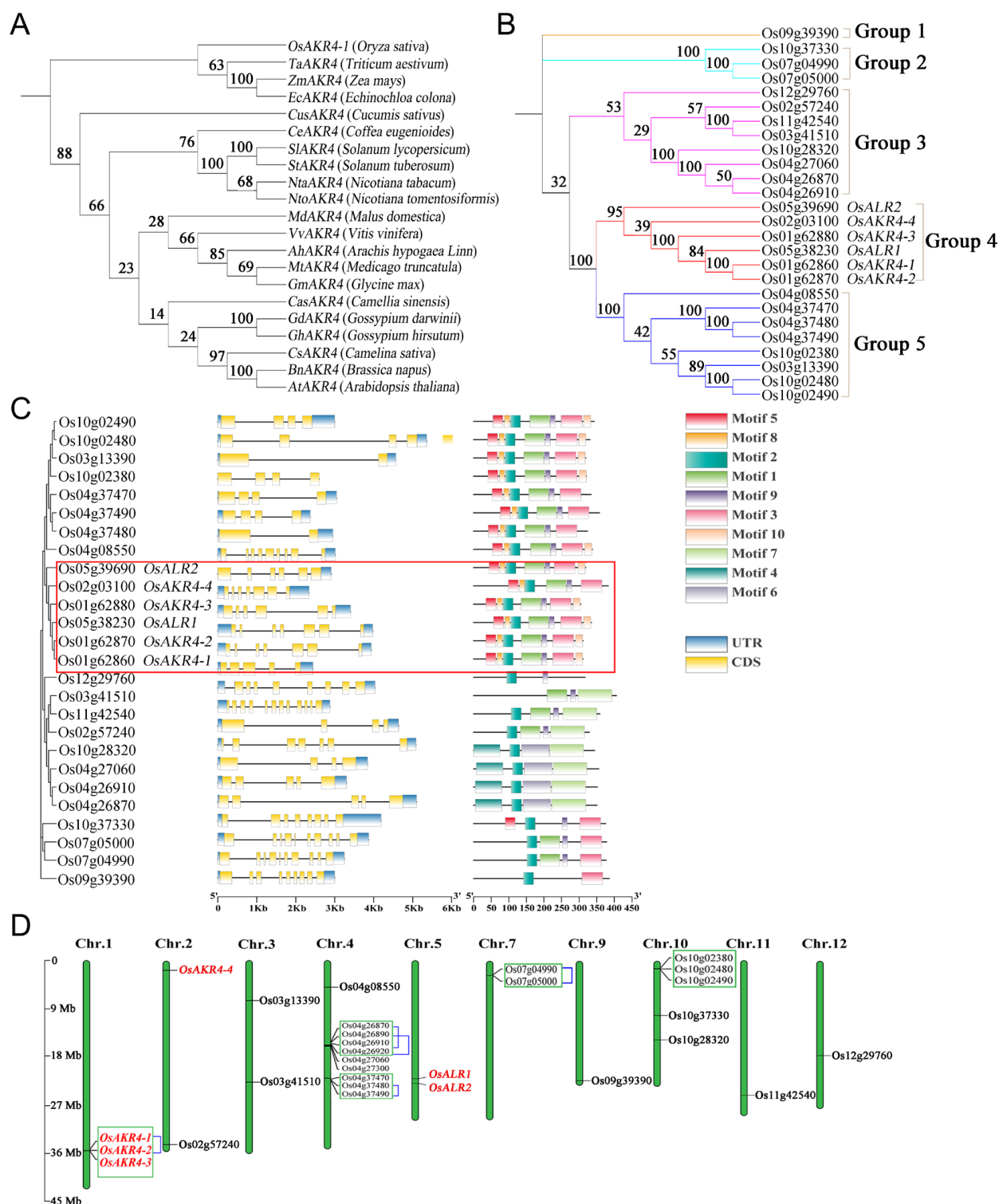


Figure 1. Bioinformatic analysis of AKR-family proteins. (A) Phylogenetic tree constructed from the amino acid sequences of the AKR4 family in 21 plants. (B) Phylogenetic tree constructed from the amino acid sequences of OsAKRs. The sequences to be aligned were confirmed using SMART (<http://smart.embl.de/smart>, accessed on 5 March 2022) and NCBI CDD (www.ncbi.nlm.nih.gov/cdd/, accessed on 5 March 2022). (C) The gene structure and motif of OsAKRs. The scale at the bottom represents the number of nucleotides or amino acids. (D) Distribution of OsAKRs among the rice chromosomes. The genes in the green box represent tandem-duplicated genes. The large-fragment duplication event occurs in the genes connected with blue lines.

The structures of the *OsAKR4* genes were analyzed by comparing the genomic DNA sequence and the predicted cDNA sequence. The number of exons of the *OsAKR4* genes ranged from 2 to 12. Motif 2 was present in all *OsAKR* family members, except *Os03g41510*. The reported sites, namely Tyr-49, Lys-78, and Trp-112, which play critical roles in the interaction between glyphosate and *EcAKR4* [22], were located at motifs 5, 8 and 2, respectively. All members in Group 4 contained the three conserved binding sites, implying that they may be involved in glyphosate metabolism, like the *EcAKR4* functions (Figures 1C and S1).

Gene-mapping analysis also showed that the *OsAKR4* genes were distributed unevenly on the rice genome. The largest gene cluster contained nine *OsAKRs* located on chromosomes 4 of rice with three duplication events, and the other two clusters were on chromosomes 1 and 10, which contained three genes for each. Three genes belonging to Group 4, that is, *OsAKR4-1*, *OsAKR4-2* and *OsAKR4-3*, were clustered on chromosome 1, with a large-fragment duplication event occurring between *OsAKR4-1* and *OsAKR4-2* (Figure 1D).

The six *OsAKRs* belonging to Group 4 were detected on chromosomes 1, 2, and 5. *OsAKR4-1*, *OsAKR4-2*, and *OsAKR4-3* were tandem-duplicated genes located on chromosome 1, whereas *OsALR1* and *OsALR2* were neighbours on chromosome 5, and *OsAKR4-4* was singly mapped to chromosome 2. These results implied that the *OsAKR* family arises from tandem duplication and gene duplications of a large chromosomal region. Most *OsAKRs* may originate from common ancestors, which accounts for the functional conservation.

2.2. AKR-Expressing *E. coli* Cells Acquire Tolerance to Glyphosate

To explore the *AKRs* that directly impart glyphosate tolerance in plants, we introduced *AKRs* into *E. coli* BL21 and examined its growth in the presence of glyphosate (Figure 2). The growth of *E. coli* harbouring the pET32a empty vector was impaired in media containing glyphosate, whereas the *E. coli* transfected with vectors harbouring *AKR4s* from *E. colona*, maize, soybean and rice exhibited stronger growth. Specifically, when cultured in 2.0 or 2.5 mg/mL glyphosate for 14 h, *E. coli* expressing *ZmAKR4* and *OsAKR4-1* showed the highest growth, while *ZmAKR4* or *GmAKR4*-expressing *E. coli* showed greater growth than the other strains when incubated with 3 mg/mL glyphosate (Figure 2A–C).

In addition, *E. coli* strains carrying rice *AKRs* (*OsAKR4-1*, *OsAKR4-2*, *OsAKR4-3*, *OsAKR4-4*, *OsALR1* and *OsALR2*) conferred varying degrees of sensitivity to glyphosate (Figure 2D–F). Moreover, pET32a-*OsAKR4-1* and *OsAKR4-4* carrying strains had remarkably higher growth than the pET32a empty vector under incubation with 2.0 or 2.5 mg/mL glyphosate. When the glyphosate concentration was increased to 3 mg/mL, *E. coli* strains expressing *OsAKR4-1* and *OsAKR4-3* exhibited high survival. In contrast, *E. coli* harbouring *OsALR1* exhibited an equivalent or even high-sensitivity phenotype to 3 mg/mL glyphosate, which was consistent with the finding that *OsALR1* did not metabolize glyphosate [21]. Taken together, these findings indicated that *AKRs*, except *OsALR1*, endowed glyphosate tolerance in an *E. coli* system, with *ZmAKR4* leading to the highest tolerance among all *AKRs*, and *OsAKR4-1* exhibited the highest tolerance among the six *OsAKRs* in rice.

2.3. AKR Protein Expression and Substrate Activity

AKR superfamilies typically use NADP⁺/NADPH as a co-factor to perform the catalytic reaction of aldehydes and ketones, sugar, and other specific substrates [26,37–39]. The changes in NADPH-absorbance level serve as an indicator for the metabolic activity of *AKR* proteins on their corresponding substrates. In this study, *AKR* proteins were purified using a Ni-NTA column from cell lysis of *E. coli* strains expressing *AKRs* at 16 °C, induced by 0.25 mM IPTG. The SDS-PAGE analysis revealed the successful expression of the proteins. The *EcAKR4* protein showed a molecular mass of approximately 40 kD (kilo Dalton) [22], whereas the other *AKRs* were about 50 kD, consistent with the predicted molecular weight (Figure S2). The efficiency of *AKR* proteins in catalyzing the degradation of benzaldehyde and glyphosate was evaluated. With benzaldehyde as a substrate,

GmAKR4 displayed the strongest degradation activity ($V_{\max} = 155.14 \pm 5.6 \text{ nmol mg}^{-1} \text{ min}^{-1}$) among the AKR proteins tested (Figure 3A,C). Among the OsAKRs, OsAKR4-2 led to the largest reduction in $A_{340\text{nm}}$ value, whereas OsAKR4-4 and OsALR2 did not cause any change (Figure 3B). Furthermore, enzyme kinetic curves were plotted for each AKR protein by conducting enzymatic reactions under a concentration gradient. GmAKR4 showed the lowest K_m value, suggesting that its benzaldehyde degradation ability was the highest among AKRs. Among OsAKRs, OsAKR4-1 and OsAKR4-2 exhibited high degradation activity on benzaldehyde. Moreover, the K_{cat}/K_m ratio was calculated for evaluating the catalytic efficiency and the result was similar to K_m result, in which GmAKR4 had the highest activity among all AKRs, and OsAKR4-1 and OsAKR4-2 in OsAKRs were the most efficient OsAKR for metabolizing benzaldehyde (Figures 3C and S3).

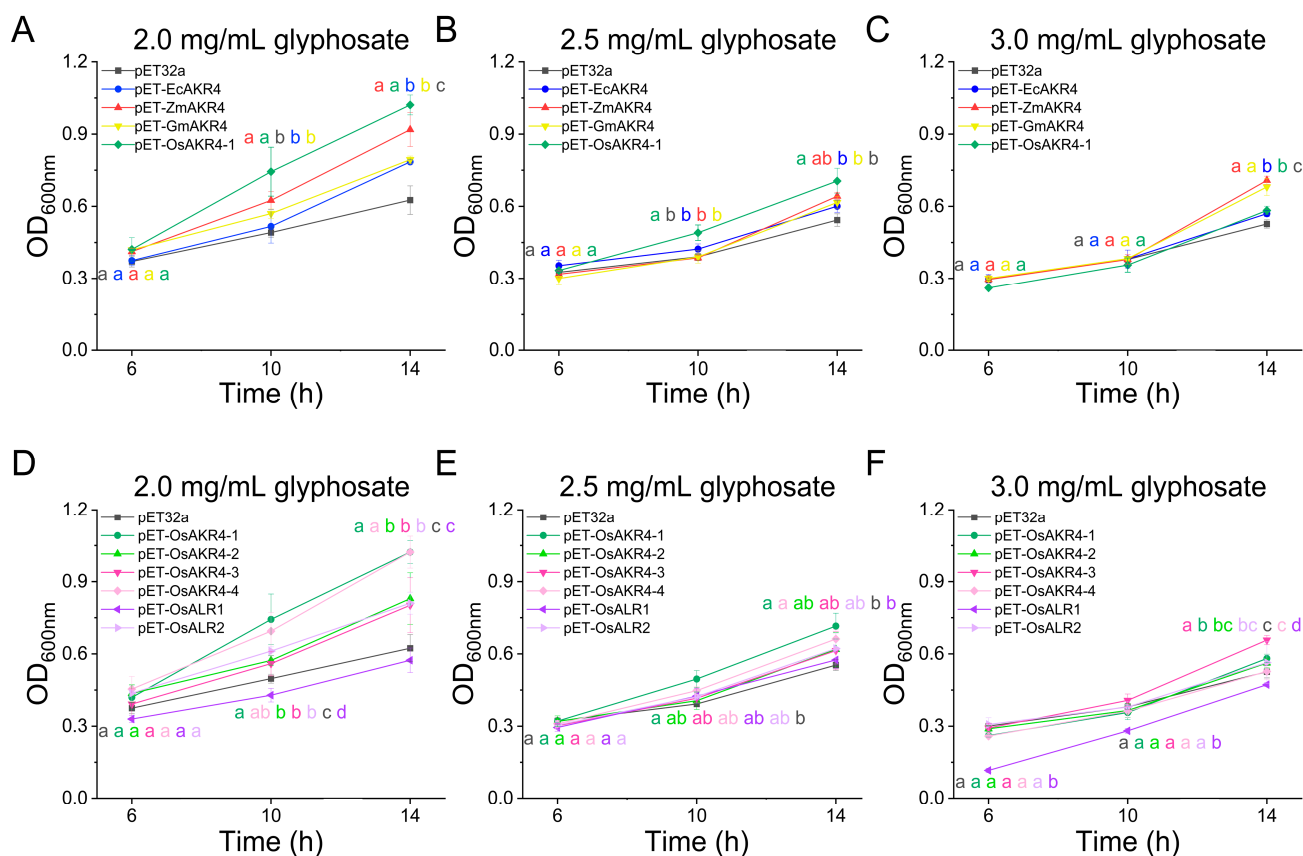


Figure 2. Growth of *Escherichia coli* BL21 expressing pET32a empty vector and pET32a-AKR in the presence of glyphosate. (A–C) *E. coli* growth curves plotted at $OD_{600\text{nm}}$ influenced by *EcAKR4*, *ZmAKR4*, *GmAKR4* and *OsAKR4-1*. The cells were grown in a liquid medium containing 2.0 mg/mL (A), 2.5 mg/mL (B) or 3.0 mg/mL (C), of glyphosate. (D–F) *E. coli* growth curves plotted at $OD_{600\text{nm}}$ influenced by AKRs from rice (*OsAKR4-1*, *OsAKR4-2*, *OsAKR4-3*, *OsAKR4-4*, *OsALR1* and *OsALR2*). The cells were grown in a liquid medium containing 2.0 mg/mL (D), 2.5 mg/mL (E), or 3.0 mg/mL (F), of glyphosate. Data are mean \pm standard deviation. $n = 3$. ($p < 0.05$; Duncan's multiple range tests).

Unlike benzaldehyde to be hydrolyzed, glyphosate is typically oxidized by AKR proteins, with a similar degradation mechanism to that of 5α -dihydro-testosterone and xylitol [25,31,40]. This reaction induced the conversion of NADP^+ to NADPH , leading to an increase in the $A_{340\text{nm}}$ value. Evaluation of the enzyme reaction showed that with glyphosate as a substrate, the enzyme activity ranking was as follows: $\text{ZmAKR4} > \text{EcAKR4} > \text{OsAKR4-1} > \text{GmAKR4}$ (Figure 4A(i)). *ZmAKR4*-expressing *E. coli* showed the highest glyphosate tolerance, as indicated by the detoxification of most of the glyphosate (Figure 2A–C). Previous studies revealed that *ZmAKR4* preferred the conversion of sor-

bitol to glucose in the reaction (sorbitol + NADP⁺ ⇌ glucose + NADPH) [31,41]. Therefore, ZmAKR4 appeared to favour using NADP⁺ to oxidize glyphosate, rather than using NADPH to reduce benzaldehyde.

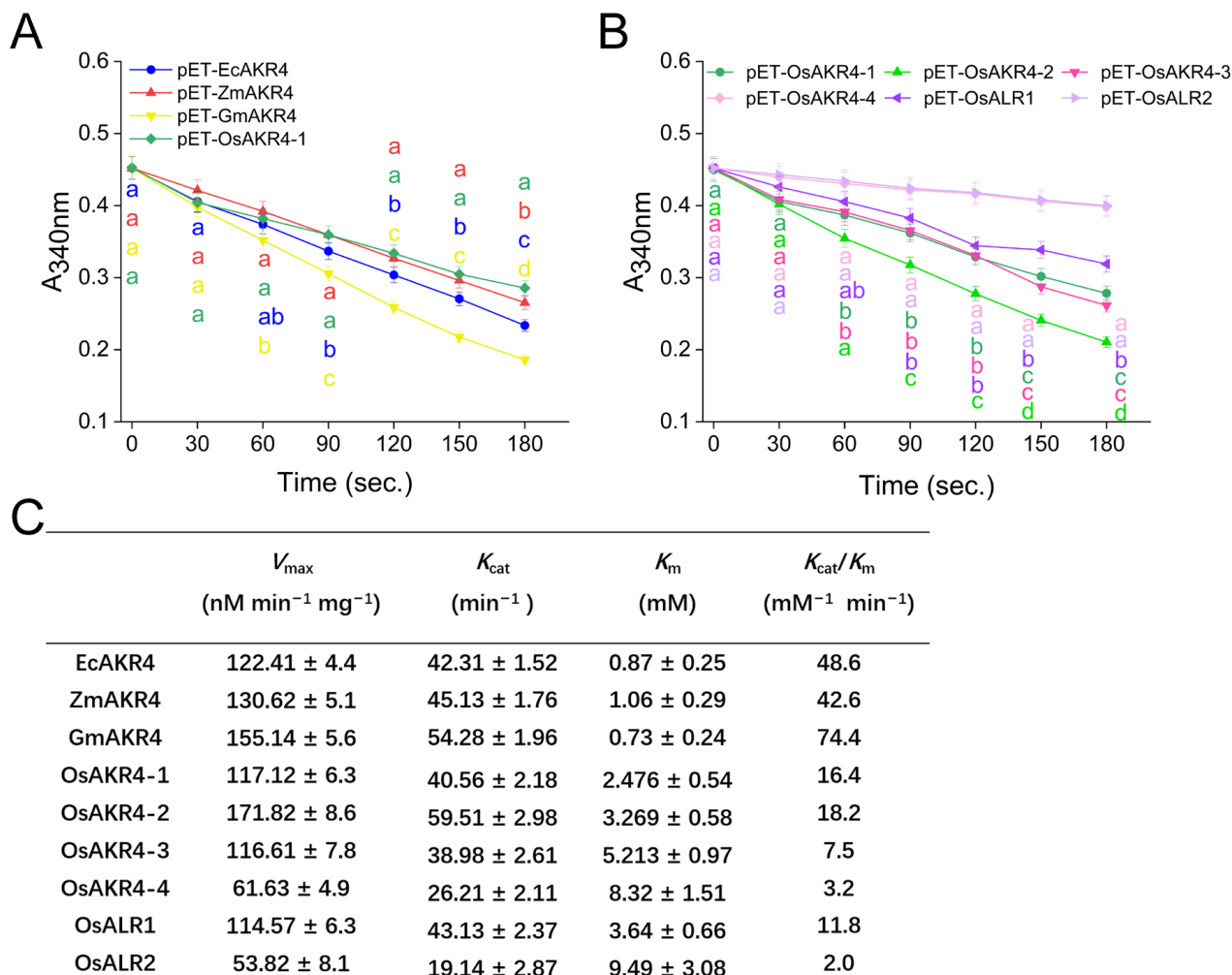


Figure 3. Activity of purified AKR proteins against benzaldehyde in vitro. (A,B) Enzyme activity of EcAKR4, ZmAKR4, GmAKR4, and OsAKR4-1 (A) along with OsAKRs (B) against 10 mM benzaldehyde. (C) Kinetic parameters of benzaldehyde metabolism by AKR enzymes. Data are mean ± standard deviation, $n = 3$.

To further investigate the binding site between AKRs and glyphosate, molecular-docking analysis was performed. Glyphosate formed a conventional hydrogen bond with Trp-21, Try-49, His-111, Trp-112, Ser-154 and Asn-155 of ZmAKR4, as well as NADP⁺. Trp-21 also contacted with glyphosate by pi-cation and pi-donor hydrogen bond (Figure 4C(i)). GmAKR4 directly occupied the Ser-207, Pro-208, Leu-209, Ser-211, Leu-254, and Lys-256 amino acid sites (Figure 4C(ii)). For OsAKR4-1, its Trp-21, His-111, and Trp-112 residues directly contacted with glyphosate by pi-cation, the conventional hydrogen bond and the pi-donor hydrogen bond, respectively (Figure 4C(iii)). Moreover, Van Der Waals (VDW) interactions were also formed among glyphosate and the surrounding residues of ZmAKR4, GmAKR4 or OsAKR4-1. All of these above interactions contribute to the binding energy between glyphosate and these three AKR proteins.

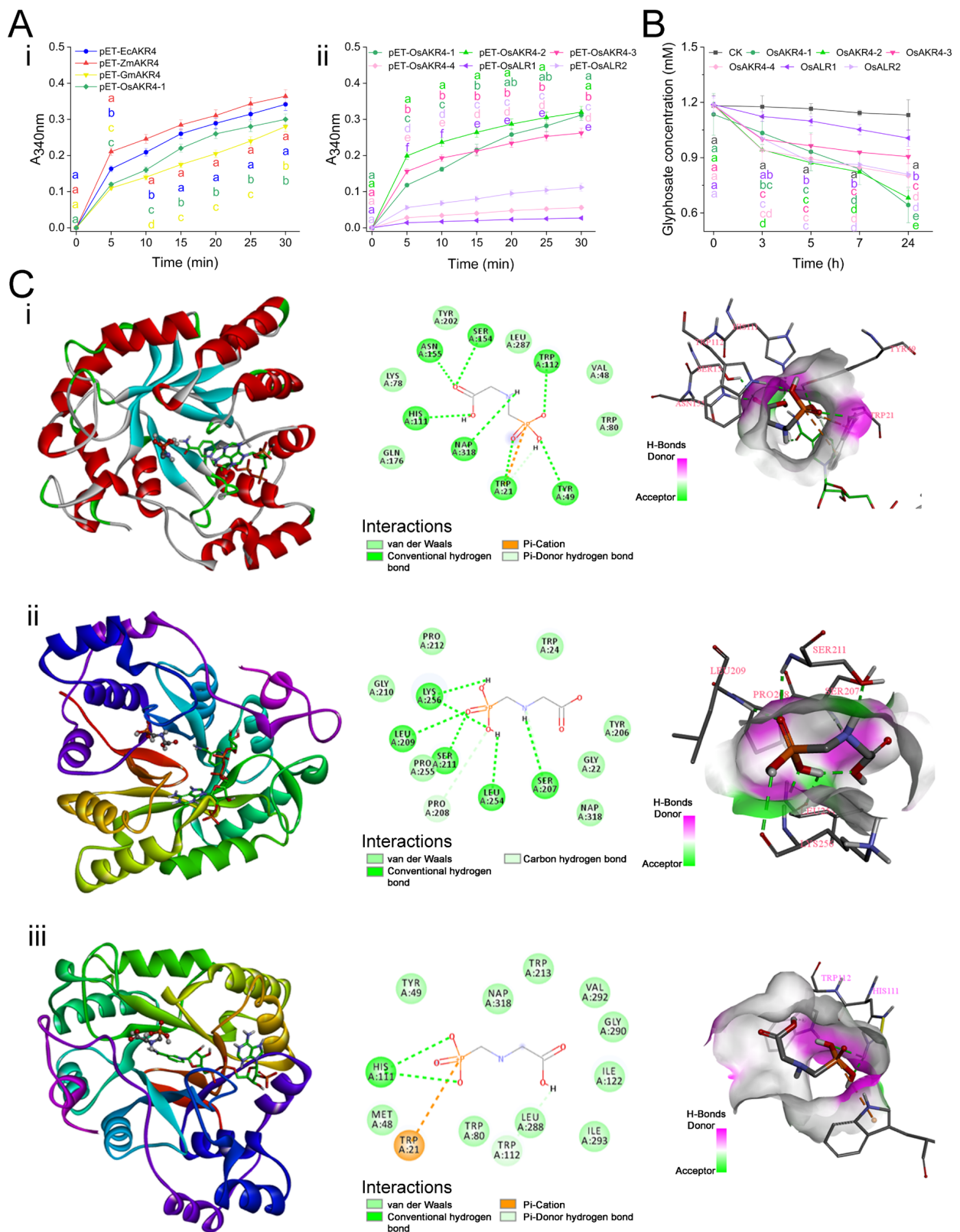


Figure 4. Comparison of the glyphosate-metabolism activities of AKR proteins. (A) Activity of purified EcAKR4, ZmAKR4, GmAKR4, OsAKR4-1 (i) and OsAKRs (ii) against glyphosate in vitro. Data are mean \pm standard deviation, $n = 3$. (B) UPLC-MS/MS analysis of glyphosate metabolized by *E. coli*-expressed OsAKRs. (C) Molecular docking of NADP⁺ complexes with ZmAKR4 (i), GmAKR4 (ii), and OsAKR4-1 (iii) with glyphosate.

2.4. OsAKR Proteins Are Involved in Glyphosate Metabolism

The glyphosate-degradation activities of OsAKRs were evaluated by comparing glyphosate-metabolism rates in AKR-expressing *E. coli*. The results showed that OsAKR4-1 and OsAKR4-2 had the highest reaction with glyphosate, whereas OsALR1 showed the lowest activity (Figure 4A(ii)).

The ability of OsAKRs to metabolize glyphosate was further evaluated by co-incubation analysis of glyphosate with the purified proteins *in vitro*. Glyphosate metabolism did not occur in the controls at all time points, while the glyphosate content decreased after incubation with OsAKR proteins. Compared with those in the control, glyphosate concentrations were 56.8%, 60.3%, 80.0%, 70.8%, 88.9%, and 71.6% after treatment for 24 h in *OsAKR4-1*, *OsAKR4-2*, *OsAKR4-3*, *OsAKR4-4*, *OsALR1* and *OsALR2*, respectively (Figure 4B). This result provided evidence that OsAKR4-1 and OsAKR4-2 had the highest glyphosate-metabolizing capacity among all OsAKRs. However, the degree of glyphosate degradation was low in the *OsALR1*-expressing *E. coli* system. A possible cause was that OsAKR4-1 could bind and catalyze glyphosate more efficiently than OsALR1, as demonstrated by molecular docking and dynamic analyses [21]. In addition, conserved Trp-21 was the binding site of glyphosate, but sequence alignment revealed that OsALR1 carried Ser in the Trp-21 site (Figure S4). Overall, ZmAKR4, OsAKR4-1 and OsAKR4-2 exhibited the highest glyphosate-degradation activity among the AKRs tested. They were also assembled in a subclade sharing, with *OsAKR4-2* sharing the most sequence identity (89%) with *OsAKR4-1* (Figure 1). This finding implies that the function of AKRs is conserved throughout its evolution.

2.5. The Response of OsAKRs in Rice Seedlings to Glyphosate Treatment

To investigate how the OsAKRs cooperate in response to glyphosate treatment, their expression patterns were monitored. The expression of most OsAKRs was induced by glyphosate treatment at a specific time point, except that of *OsALR1*, which showed no glyphosate-degradation function either *in vivo* or *in vitro*. The expression of both *OsAKR4-1* and *OsAKR4-2* in rice was induced by glyphosate treatment in a short time (5 h), with *OsAKR4-1* expression dramatically increasing at the 72 h time point, suggesting its critical role in the degradation of glyphosate. *OsAKR4-3* and *OsAKR4-4* expression was also upregulated to varying degrees at the mid-stage. Interestingly, a decrease in *OsALR1* expression was observed in the period of glyphosate spraying (Figure 5). These data indicate that OsAKR4-1 is a key enzyme for rice in glyphosate metabolism with working continuously.

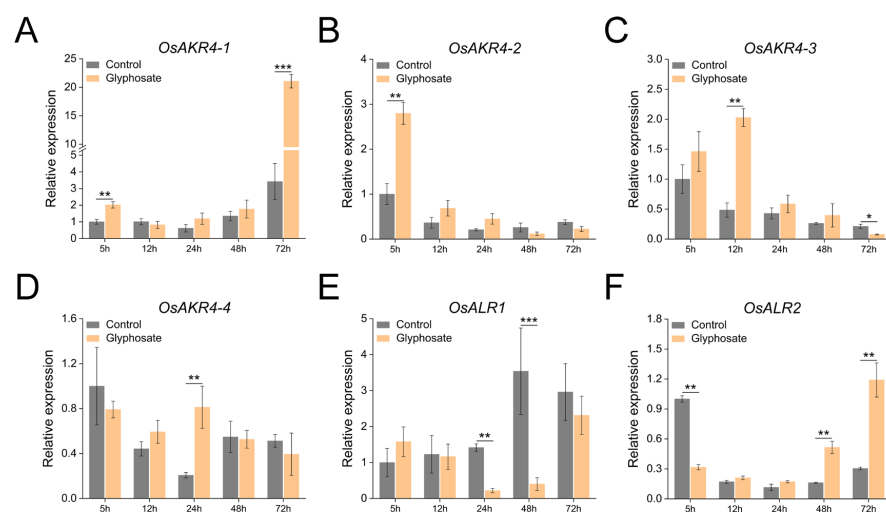
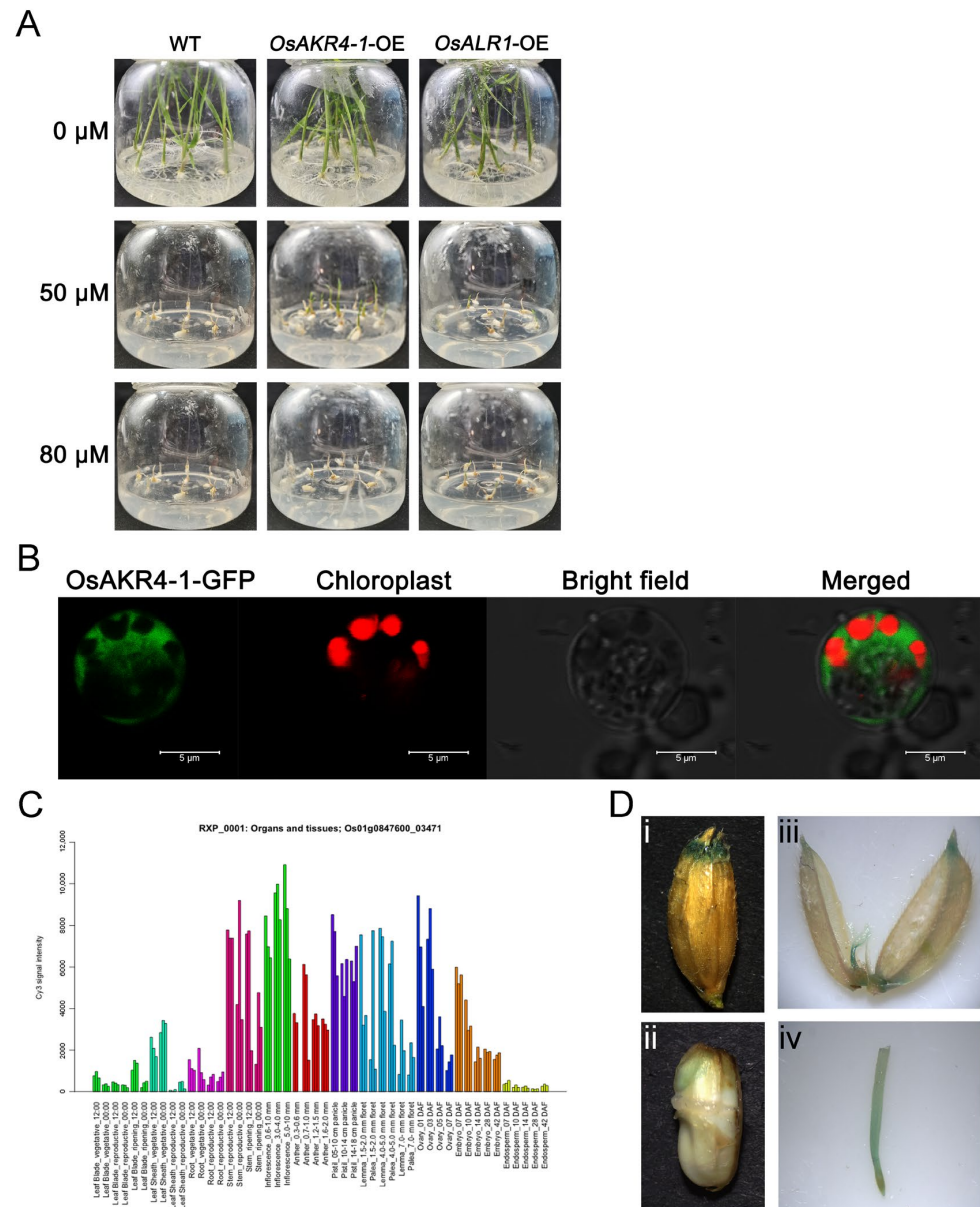


Figure 5. Transcription profiles of OsAKRs in response to glyphosate treatment. (A) for *OsAKR4-1*. (B) for *OsAKR4-2*. (C) for *OsAKR4-3*. (D) for *OsAKR4-4*. (E) for *OsALR1*. (F) for *OsALR2*. Two-week-old rice seedlings were sprayed with 13 mM glyphosate, and RNA was extracted from the shoots at 5, 12, 24, 48, and 72 h after treatment. Data are mean \pm standard deviation, $n = 3$. (* $p < 0.05$, ** $p < 0.01$, *** $p < 0.001$; Duncan's multiple range tests).

To further address the role of *OsAKR4-1* in response to glyphosate, we examined the phenotype of rice overexpressing *OsAKR4-1* and *OsALR1* under glyphosate stress (Figure S5). Glyphosate can lead to the inhibition of seedling growth and cause seedling wilting and browning. In our seed-germination experiment, the damage to the seedling was more pronounced in the wild type and *OsALR1*-OE than in the *OsAKR4-1*-OE under 50 μM glyphosate, whereas they showed similar inhibited growth in high-concentration glyphosate (80 μM) (Figure 6A). This result further validated the fact that *OsAKR4-1* was a critical factor in metabolizing glyphosate but *OsALR1* was not.



2.6. Localization of OsAKR4-1 in Rice

The signal of GFP-tagged OsAKR4-1 was localized in the cytoplasm, suggesting that the cytoplasm was the site of glyphosate metabolism by OsAKR4-1 (Figure 6B). Expression-pattern analysis showed that *OsAKR4-1* was mainly expressed in the stem, floral organs and seed ovary and embryo (Figure 6C); this finding resembles the result of the tissue-localization analysis. GUS-staining signals driven by *OsAKR4-1* promoter were detected at the glume, embryo, lemma and root (Figure 6D), illustrating that *OsAKR4-1* played an important role in seed germination and pollen development. Although OsAKR4-1 could degrade 43.9% of glyphosate, this ability was not as strong as that of EcAKR4 (92.5%) (Figure S6). It was observed that only OsAKR4-1 was not enough to endow excellent glyphosate resistance in rice (Figures 4B and 6A). This observation was reasonable, as EcAKR4 conferred glyphosate resistance only in plants harboring the EPSPS target mutation [42]. Therefore, it is reasonable to infer that *OsAKR4-1* can be coupled with the target gene to provide herbicide resistance in rice for commercial production. The advantages of such a strategy lie in improving glyphosate resistance while reducing glyphosate residue in crops [5,43,44].

3. Materials and Methods

3.1. Sequence Homology among Different Plants

To study the relationship of the AKR family among plants that are often exposed to glyphosate, the amino acid sequences of 21 plants were retrieved from NCBI (<https://www.ncbi.nlm.nih.gov/>, accessed on 5 March 2022) for phylogenetic analysis. The plants included *Arabidopsis thaliana* (AT2G37790), *Arachis hypogaea* Linn (LOC112727795), *Brassica napus* (LOC106451053), *Camelina sativa* (LOC104785711), *Camellia sinensis* (LOC114297399), *Coffea eugenioides* (LOC113772474), *Cucumis sativus* (LOC101209936), *Echinochloa colona* (MK592097), *Glycine max* (LOC100802323), *Gossypium darwinii* (TYH22311), *Gossypium hirsutum* (LOC107888724), *Malus domestica* (LOC103450273), *Medicago truncatula* (LOC25501528), *Nicotiana tabacum* (LOC107767146), *Nicotiana tomentosiformis* (LOC104097840), *Oryza sativa* (LOC4327475), *Solanum lycopersicum* (LOC101256514), *Solanum tuberosum* (LOC102593301), *Triticum aestivum* (KAF7024607.1), *Vitis vinifera* (LOC100254427) and *Zea mays* (LOC100037812). A total of 21 sequences were aligned, using ClustalW version 2.1. Next, the sequences were grouped through neighbour-joining analysis with 1000 bootstrap replicates using MEGA version 7.0. Phylogenetic trees were drawn using iTOL (<https://itol.embl.de/>, accessed on 5 March 2022).

The OsAKR4-1 (LOC4327475) protein sequence from rice was submitted to the Pfam (<http://pfam.xfam.org>, accessed on 5 March 2022) to construct a hidden Markov model (HMM), and matching sequences were obtained using the hmmsearch program. The representative sequences were confirmed using SMART (<http://smart.embl.de/smart>, accessed on 5 March 2022) and NCBI CDD (www.ncbi.nlm.nih.gov/cdd/, accessed on 5 March 2022) and then used for phylogenetic analysis, as mentioned before. Moreover, the protein sequences of OsAKRs were submitted to the MEME database (<http://meme.nbcr.net/meme/intro.html>, accessed on 5 March 2022) to find conserved motifs, searching for up to 10 motifs. Comparative analysis of exon–intron gene structures for OsAKRs was conducted by GSDS (<http://gsds.cbi.pku.edu>, accessed on 5 March 2022). Finally, the physical map of the chromosome was visualized using the MapChart software (ADInstruments, Newcastle, Australia).

3.2. Cloning Procedure and Plasmid Construction

EcAKR4, *ZmAKR4*, *GmAKR4* and OsAKRs (*OsAKR4-1*, *OsAKR4-2*, *OsAKR4-3*, *OsAKR4-4*, *OsALR1* and *OsALR2*) were selected for further analysis. The coding sequence (CDS) of these candidate AKR genes was amplified (Table S2) using the cDNA from plant leaves as a template and then cloned into the *pEASY-Blunt* cloning vector (Transgen, Beijing, China) following the manufacturer's instruction. However, the CDS of *GmAKR4* and *OsALR1* could not be amplified, and thus were chemically synthesized by BGI (BGI, Beijing, China).

Subsequently, the target genes were sub-cloned into the expression vector pET32a, using the in-fusion method (Takara, Dalian, China). All recombinant vectors were sequenced, to confirm that the inserts were correct.

3.3. Expression and Purification of AKRs in *E. coli*

The resulting pET32a-*EcAKR4*, *ZmAKR4*, *GmAKR4*, and *OsAKRs* constructs were transferred into the *E. coli* BL21 as the expression host. The cells were grown on an LB solid medium containing ampicillin (Amp) for 10 h, at 37 °C. The colonies were then cultured in an LB liquid medium (Amp⁺), with shaking at 200 rpm. When the OD₆₀₀ reached 0.6–0.8, IPTG was added at a final concentration of 0.25 mM. Cells were grown at 16 °C for 16 h to induce the expression of target proteins. Next, the cells were harvested by centrifugation at 6000 × g at 4 °C for 10 min, resuspended in a lysis buffer (25 mM Tris-HCl pH 7.5, 300 mM NaCl, and 20 mM imidazole), and then disrupted using a high-pressure cell cracker at 1500 bar. Cell debris was discarded by centrifugation at 11,000 × g at 4 °C for 30 min. The supernatant was applied to an Ni-NTA column that had been equilibrated with five column volumes of lysis buffer. Other proteins were removed using wash buffer (25 mM Tris-HCl pH 7.5, 300 mM NaCl, and 70 mM imidazole), and bound proteins were eluted using an elution buffer (20 mM Tris-HCl pH 8.0, 300 mM NaCl, and 300 mM imidazole). The purity of the protein was determined by 12% SDS-PAGE analysis and then stored at –80 °C, with glycerin added.

3.4. Comparative-Growth Test of Glyphosate in *E. coli*

Briefly, *E. coli* containing the pET32a gene were shake-cultured in an LB medium (Amp⁺) for 4 h, and IPTG was added at a final concentration of 1 μM, followed by the addition of glyphosate at various concentrations (2, 2.5 and 3 mg/mL). The cultures were then incubated with shaking at 180 rpm and 37 °C. The OD₆₀₀ of each culture was monitored at 6, 10 and 14 h for plotting the OD₆₀₀-growth-time function.

3.5. Measurement of Enzyme Activity in *E. coli*

AKR activities in *E. coli* were measured as described previously, with modification [23]. For experiments using benzaldehyde as a substrate, the reaction mixture (1 mL) contained 50 mM phosphate buffer (pH 7.4), 0.1 mM NADPH, 10 mM β-mercaptoethanol, 100 μg purified protein and 10 mM benzaldehyde. In the enzyme kinetic analysis, the concentration of benzaldehyde in the reaction mixture was set to 2.5, 5.0, 7.5, 10, 15 and 20 mM. For experiments using glyphosate as a substrate, the reaction mixture (1 mL) contained 75 mM Tris-HCl buffer (pH 8.6), 0.1 mM NADP⁺, 10 mM β-mercaptoethanol, 20 μg purified protein, and 0.5 mM glyphosate. All reactions proceeded at 25 °C for different durations (up to 3 min for benzaldehyde and up to 30 min for glyphosate). The enzyme activity was confirmed according to the absorbance of NADPH at 340 nm, as measured using a biophotometer (Eppendorf, Germany).

3.6. Degradation of Glyphosate by *E. coli*

The purified *OsAKR* proteins were used for catalyzing the glyphosate degradation. In the reaction mixture, 20 μg purified protein was cultured with excessive 0.1 mM NADP⁺, 0.5% Tween 80 and 1.48 mM glyphosate in the 75 mM Tris-HCl buffer at pH 6.8 and 35 °C for different durations (0, 3, 5, 7, and 24 h). Mixtures without AKR protein were treated as controls. The UPLC-MS/MS analysis was performed to determine the content of derivatized glyphosate in the mixture.

3.7. Molecular Docking of AKRs with Glyphosate

The spatial structures of *ZmAKR4*, *GmAKR4*, and *OsAKR4-1* were downloaded from the AlphaFold Protein Structure Database (<https://alphafold.com/>, accessed on 3 July 2022) [45,46]. The NADP⁺-bound AKRs were used for molecular docking with glyphosate. The binding pocket of *ZmAKR4*, *GmAKR4*, and *OsAKR4-1* were set to be center

$x/y/z = 8.487/-0.624/-0.572$, $5.308/6.165/5.503$ and $5.176/9.278/-2.137$, respectively. Docking was performed in the AutoDock Vina, followed by preparation of the three-dimensional graphics using Discovery Studio.

3.8. Measurement of Glyphosate Using UPLC-MS/MS

The samples were reacted with 9-fluorenylmethoxycarbonyl chloride (Fmoc-Cl) (1.0 g/L in acetone) in a sodium borate buffer (50.0 g/L, pH 9) at 37 °C for 10 h, to generate Fmoc-derivative products. UPLC-MS/MS analysis was performed using a Xevo TQD mass spectrometer (Waters, Milford, MA, USA) interfaced with ACQUITY UPLC[®] H-Class system. The samples were separated by an ACQUITY UPLC BEH C18 (2.1 × 100 mm, 1.7 μm, Waters), with acetonitrile and 2 mM ammonium acetate water with 0.1% formic acid as the mobile phase. The following instrument parameters were used: desolvation temperature, 550 °C; cone voltage, 25 V; capillary voltage, 500 V. The MS/MS ion transitions and collision energy for compounds were as follows: glyphosate, ESI⁺, m/z 392.1-88 (25 eV), 170 (12 eV), and 214 (12 eV).

3.9. Gene-Expression Analysis Using qRT-PCR

Rice seedlings were grown in modified Hoagland nutrient solutions for 2 weeks, and later sprayed with 13 mM glyphosate. RNA was isolated from the shoots at 5, 12, 24, 48 and 72 h after treatment, and subjected to qRT-PCR analysis for monitoring the expression of OsAKRs.

3.10. Glyphosate-Tolerance Seed-Germination Assay

The promoter sequences of *OsAKR4-1* and *OsALR1* were amplified by PCR and cloned into the pCAMBIA1300-35S vector with 35S promoter. Then they were transformed into Zhonghua11 by *Agrobacterium tumefaciens*-edited transformation to generate *OsAKR4-1*-OE and *OsALR1*-OE lines, which were confirmed by gene-expression-level analysis, using qRT-PCR. For observing the resistance to glyphosate, the seeds of *OsAKR4-1*-OE and *OsALR1*-OE lines were germinated on MS medium supplemented with 50 or 80 μM glyphosate for 2 weeks, and photographed.

3.11. Subcellular Localization of OsAKR4-1

To detect the localization of OsAKR4-1, the OsAKR4-1-GFP plasmid was transfected into the rice protoplast for screening the fluorescence signal, using a Leica SP8 confocal laser scanning microscope as the parameter mentioned previously [47].

3.12. Histochemical Determination of GUS Activity

Germinating rice seeds, the root, stem and leaf of 2-week-old seedlings, and rice florets at the flowering stage were stained using a GUS solution kit (Coolaber, Beijing, China). In brief, all tissues were incubated overnight at 37 °C and then cleared in the 70% ethanol. The GUS-staining results were observed using a stereoscope, as described previously [47].

4. Conclusions

Glyphosate is an efficient broad-spectrum herbicide widely used in agricultural production. The cultivation of transgenic glyphosate-resistant crops has significantly increased the easy use of glyphosate, in which the crops endowed metabolic resistance, is being considered. Previous studies have shown that AKR in *E. colona* has the function of degrading glyphosate. In this study, we compared the effectiveness of AKRs from maize, soybean, and rice with that of EcAKR4 in metabolizing glyphosate. All these proteins have emerged as novel enzymes for glyphosate degradation, with ZmAKR4 showing the highest activity. Moreover, OsAKR4-1 and OsAKR4-2 exhibited excellent glyphosate-metabolizing capacity (among six OsAKRs), and *OsAKR4-1* provided continuous response to glyphosate in plants so, that the rice with overexpressed *OsAKR4-1* had a degree of resistance to

glyphosate. Thus, we demonstrate these genes as potential candidates for cultivating glyphosate-resistant crops with low glyphosate residue.

Supplementary Materials: The following supporting information can be downloaded at <https://www.mdpi.com/article/10.3390/ijms24043421/s1>.

Author Contributions: Conceptualization, F.L. and H.X.; data curation, R.C., S.W. (Siwei Wang), Y.S. and H.L.; investigation, R.C., S.W. (Siwei Wang) and S.W. (Shuqing Wan); methodology, R.C., S.W. (Siwei Wang), Y.S., H.L., S.W. (Shuqing Wan), F.L. and H.X.; project administration, F.L. and H.X.; software, R.C.; supervision, F.L. and H.X.; writing—original draft, R.C. and S.W. (Siwei Wang); writing—review and editing, F.L. and H.X. All authors have read and agreed to the published version of the manuscript.

Funding: This work was funded by the Guangdong Modern Agricultural Industry Generic Key Technology Research and Development Innovation Team Project (Grant No. 2020KJ133), the Generic Technique Innovation Team Construction of Modern Agriculture of Guangdong Province (2022KJ130), the Project of Science and Technology in Guangdong Province (Grant No. 2018A030313188), and the Science and Technology Planning Project of Guangdong Province (2019B030316021).

Institutional Review Board Statement: Not applicable.

Informed Consent Statement: Not applicable.

Data Availability Statement: Not applicable.

Acknowledgments: We acknowledge the guidance of Zhiming Zhang (School of Pharmacy, Jinan University) and Guowei Yin (The Seventh Affiliated Hospital, Sun Yat-sen University) for the AKR prokaryotic-protein expression and purification, and Yinghua Wu and Guodong Liao (Zhong Shan Lan Ju Daily Chemical Industrial Co., Ltd.) for providing some measuring instruments and support for this research project.

Conflicts of Interest: The authors declare no conflict of interest.

References

1. Duke, S.O.; Powles, S.B.; Sammons, R.D. Glyphosate—How it became a once in a hundred year herbicide and its future. *Outlooks Pest Manag.* **2018**, *29*, 247–251. [[CrossRef](#)]
2. Padgett, S.R.; Kolacz, K.H.; Delannay, X.; Re, D.B.; LaVallee, B.J.; Tinius, C.N.; Rhodes, W.K.; Otero, Y.I.; Barry, G.F.; Eichholtz, D.A. Development, identification, and characterization of a glyphosate-tolerant soybean line. *Crop. Sci.* **1995**, *35*, 1451–1461. [[CrossRef](#)]
3. Tan, S.; Evans, R.; Singh, B. Herbicidal inhibitors of amino acid biosynthesis and herbicide-tolerant crops. *Amino Acids* **2006**, *30*, 195–204. [[CrossRef](#)] [[PubMed](#)]
4. Duke, S.O.; Powles, S.B. Glyphosate: A once-in-a-century herbicide. *Pest Manag. Sci.* **2008**, *64*, 319–325. [[CrossRef](#)]
5. Wen, L.; Zhong, J.; Cui, Y.; Duan, Z.; Zhou, F.; Li, C.; Ma, W.; Yin, C.; Chen, H.; Lin, Y. Coexpression of *I. variabilis*-EPSPS* and *WBceGO-B3S1* genes contributes to high glyphosate tolerance and low glyphosate residues in transgenic rice. *J. Agric. Food Chem.* **2021**, *69*, 7388–7398. [[CrossRef](#)]
6. Bostamam, Y.; Malone, J.M.; Dolman, F.C.; Boutsalis, P.; Preston, C. Rigid Ryegrass (*Lolium rigidum*) Populations containing a target site mutation in EPSPS and reduced glyphosate translocation are more resistant to glyphosate. *Weed Sci.* **2012**, *60*, 474–479. [[CrossRef](#)]
7. Powles, S.B.; Yu, Q. Evolution in action: Plants resistant to herbicides. *Annu. Rev. Plant Biol.* **2010**, *61*, 317–347. [[CrossRef](#)]
8. Morran, S.; Moretti, M.L.; Brunharo, C.A.; Fischer, A.J.; Hanson, B.D. Multiple target site resistance to glyphosate in junglerice (*Echinochloa colona*) lines from California orchards. *Pest Manag. Sci.* **2018**, *74*, 2747–2753. [[CrossRef](#)]
9. Pan, L.; Yu, Q.; Wang, J.; Han, H.; Mao, L.; Nyporko, A.; Maguza, A.; Fan, L.; Bai, L.; Powles, S. An ABC-type transporter endowing glyphosate resistance in plants. *Proc. Natl. Acad. Sci. USA* **2021**, *118*, e2100136118. [[CrossRef](#)]
10. Böhn, T.; Cuhra, M.; Traavik, T.; Sanden, M.; Fagan, J.; Primiticchio, R. Compositional differences in soybeans on the market: Glyphosate accumulates in Roundup Ready GM soybeans. *Food Chem.* **2014**, *153*, 207–215. [[CrossRef](#)]
11. Barry, G.; Kishore, G.; Padgett, S.; Taylor, M.; Kolacz, K.; Weldon, M.; Re, D.; Eichholtz, D.; Fincher, K.; Hallas, L. Inhibitors of amino acid biosynthesis: Strategies for imparting glyphosate tolerance to crop plants. In *Biosynthesis and Molecular Regulation of Amino Acids in Plants*; Singh, B.K., Flores, H.E., Shannon, J.C., Eds.; Springer: Rockville, MD, USA, 1992; pp. 139–145.
12. Zhou, H.; Arrowsmith, J.W.; Fromm, M.E.; Hironaka, C.M.; Taylor, M.L.; Rodriguez, D.; Pajean, M.E.; Brown, S.M.; Santino, C.G.; FRY, J.E. Glyphosate-tolerant CP4 and GOX genes as a selectable marker in wheat transformation. *Plant Cell Rep.* **1995**, *15*, 159–163. [[CrossRef](#)]

13. Correa, E.A.; Dayan, F.E.; Owens, D.K.; Rimando, A.M.; Duke, S.O. Glyphosate-resistant and conventional canola (*Brassica napus* L.) responses to glyphosate and aminomethylphosphonic acid (AMPA) treatment. *J. Agric. Food Chem.* **2016**, *64*, 3508–3513. [[CrossRef](#)]
14. Mörtl, M.; Diederichs, K.; Welte, W.; Molla, G.; Motteran, L.; Andriolo, G.; Pilone, M.S.; Pollegioni, L. Structure-function correlation in glycine oxidase from *Bacillus subtilis*. *J. Biol. Chem.* **2004**, *279*, 29718–29727. [[CrossRef](#)]
15. Pedotti, M.; Rosini, E.; Molla, G.; Moschetti, T.; Savino, C.; Vallone, B.; Pollegioni, L. Glyphosate resistance by engineering the flavoenzyme glycine oxidase. *J. Biol. Chem.* **2009**, *284*, 36415–36423. [[CrossRef](#)]
16. Nicolìa, A.; Ferradini, N.; Molla, G.; Biagetti, E.; Pollegioni, L.; Veronesi, F.; Rosellini, D. Expression of an evolved engineered variant of a bacterial glycine oxidase leads to glyphosate resistance in *alfalfa*. *J. Biotechnol.* **2014**, *184*, 201–208. [[CrossRef](#)]
17. Han, H.; Zhu, B.; Fu, X.; You, S.; Wang, B.; Li, Z.; Zhao, W.; Peng, R.; Yao, Q. Overexpression of d-amino acid oxidase from *Bradyrhizobium japonicum*, enhances resistance to glyphosate in *Arabidopsis thaliana*. *Plant Cell Rep.* **2015**, *34*, 2043–2051. [[CrossRef](#)]
18. Reddy, K.N.; Rimando, A.M.; Duke, S.O.; Nandula, V.K. Aminomethylphosphonic acid accumulation in plant species treated with glyphosate. *J. Agric. Food Chem.* **2008**, *56*, 2125–2130. [[CrossRef](#)]
19. Duke, S.O. Glyphosate degradation in glyphosate-resistant and-susceptible crops and weeds. *J. Agric. Food Chem.* **2011**, *59*, 5835–5841. [[CrossRef](#)]
20. Nandula, V.K.; Riechers, D.E.; Ferhatoglu, Y.; Barrett, M.; Duke, S.O.; Dayan, F.E.; Goldberg-Cavalleri, A.; Tétard-Jones, C.; Wortley, D.J.; Onkokesung, N.; et al. Herbicide metabolism: Crop selectivity, bioactivation, weed resistance, and regulation. *Weed Sci.* **2019**, *67*, 149–175. [[CrossRef](#)]
21. Vemanna, R.S.; Vennapusa, A.R.; Easwaran, M.; Chandrashekar, B.K.; Rao, H.; Ghanti, K.; Sudhakar, C.; Mysore, K.S.; Makarla, U. Aldo-keto reductase enzymes detoxify glyphosate and improve herbicide resistance in plants. *Plant Biotechnol. J.* **2017**, *15*, 794–804. [[CrossRef](#)]
22. Pan, L.; Yu, Q.; Han, H.; Mao, L.; Nyporko, A.; Fan, L.; Bai, L.; Powles, S. Aldo-keto reductase metabolizes glyphosate and confers glyphosate resistance in *Echinochloa colona*. *Plant Physiol.* **2019**, *181*, 1519–1534. [[CrossRef](#)] [[PubMed](#)]
23. Hyndman, D.; Bauman, D.R.; Heredia, V.V.; Penning, T.M. The aldo-keto reductase superfamily homepage. *Chem. Biol. Interact.* **2003**, *143–144*, 621–631. [[CrossRef](#)] [[PubMed](#)]
24. Mindnich, R.D.; Penning, T.M. Aldo-keto reductase (AKR) superfamily: Genomics and annotation. *Hum. Genom.* **2009**, *3*, 362–370. [[CrossRef](#)] [[PubMed](#)]
25. Simpson, P.J.; Tantitadapitak, C.; Reed, A.M.; Mather, O.C.; Bunce, C.M.; White, S.A.; Ride, J.P. Characterization of two novel aldo-keto reductases from *Arabidopsis*: Expression patterns, broad substrate specificity, and an open active-site structure suggest a role in toxicant metabolism following stress. *J. Mol. Biol.* **2009**, *392*, 465–480. [[CrossRef](#)]
26. Penning, T.M. The aldo-keto reductases (AKRs): Overview. *Chem.-Biol. Interact.* **2015**, *234*, 236–246. [[CrossRef](#)]
27. Okuda, A.; Okuda, K. Purification and characterization of delta 4-3-ketosteroid 5 beta-reductase. *J. Biol. Chem.* **1984**, *259*, 7519–7524. [[CrossRef](#)]
28. Kondo, K.H.; Kai, M.H.; Setoguchi, Y.; Eggertsen, G.; Sjoblom, P.; Setoguchi, T.; Okuda, K.I.; Bjorkhem, I. Cloning and expression of cDNA of human delta4-3-oxosteroid 5 beta-reductase and substrate specificity of the expressed enzyme. *Eur. J. Biochem.* **1994**, *219*, 357–363. [[CrossRef](#)]
29. Di Costanzo, L.; Drury, J.E.; Penning, T.M.; Christianson, D.W. Crystal structure of human liver Delta4-3-Ketosteroid 5beta-Reductase (AKR1D1) and implications for substrate binding and catalysis. *J. Biol. Chem.* **2008**, *283*, 16830–16839. [[CrossRef](#)]
30. Saito, R.; Shimakawa, G.; Nishi, A.; Iwamoto, T.; Sakamoto, K.; Yamamoto, H.; Amako, K.; Makino, A.; Miyake, C. Functional analysis of the AKR4C subfamily of *Arabidopsis thaliana*: Model structures, substrate specificity, acrolein toxicity, and responses to light and [CO₂]. *Biosci. Biotechnol. Biochem.* **2013**, *77*, 2038–2045. [[CrossRef](#)]
31. De Sousa, S.M.; Rosselli, L.K.; Kiyota, E.; Da Silva, J.C.; Souza, G.H.M.F.; Peroni, L.A.; Stach-Machado, D.R.; Eberlin, M.N.; Souza, A.P.; Koch, K.E.; et al. Structural and kinetic characterization of a maize aldose reductase. *Plant Physiol. Biochem.* **2009**, *47*, 98–104. [[CrossRef](#)]
32. Turóczy, Z.; Kis, P.; Török, K.; Cserháti, M.; Lendvai, Á.; Dudits, D.; Horváth, G.V. Overproduction of a rice aldo-keto reductase increases oxidative and heat stress tolerance by malondialdehyde and methylglyoxal detoxification. *Plant Mol. Biol.* **2011**, *75*, 399–412. [[CrossRef](#)]
33. Agrawal, C.; Sen, S.; Singh, S.; Rai, S.; Singh, P.K.; Singh, V.K.; Rai, L.C. Comparative proteomics reveals association of early accumulated proteins in conferring butachlor tolerance in three N₂-fixing *Anabaena* spp. *J. Proteom.* **2014**, *96*, 271–290. [[CrossRef](#)]
34. Agrawal, C.; Sen, S.; Yadav, S.; Rai, S.; Rai, L.C. A novel aldo-keto reductase (AKR17A1) of *Anabaena* sp. PCC 7120 degrades the rice field herbicide butachlor and confers tolerance to abiotic stresses in *E. coli*. *PLoS ONE* **2015**, *10*, e0137744. [[CrossRef](#)]
35. Li, H.; Yang, Y.; Hu, Y.; Chen, C.; Huang, J.; Min, J.; Dai, L.; Guo, R. Structural analysis and engineering of aldo-keto reductase from glyphosate-resistant *Echinochloa colona*. *J. Hazard. Mater.* **2022**, *436*, 129191. [[CrossRef](#)]
36. Leebens-Mack, J.H.; Barker, M.S.; Carpenter, E.J.; Deyholos, M.K.; Gitzendanner, M.A.; Graham, S.W.; Grosse, I.; Li, Z.; Melkonian, M.; Mirarab, S.; et al. One thousand plant transcriptomes and the phylogenomics of green plants. *Nature* **2019**, *574*, 679–685. [[CrossRef](#)]
37. Bohren, K.M.; Bullock, B.; Wermuth, B.; Gabbay, K.H. The aldo-keto reductase superfamily: cDNAs and deduced amino acid sequences of human aldehyde and aldose reductases. *J. Biol. Chem.* **1989**, *264*, 9547–9551. [[CrossRef](#)] [[PubMed](#)]

38. Burczynski, M.E.; Sridhar, G.R.; Palackal, N.T.; Penning, T.M. The reactive oxygen species-and Michael acceptor-inducible human aldo-keto reductase AKR1C1 reduces the alpha, beta-unsaturated aldehyde 4-hydroxy-2-nonenal to 1, 4-dihydroxy-2-nonenal. *J. Biol. Chem.* **2001**, *276*, 2890–2897. [[CrossRef](#)] [[PubMed](#)]
39. Sengupta, D.; Naik, D.; Reddy, A.R. Plant aldo-keto reductases (AKRs) as multi-tasking soldiers involved in diverse plant metabolic processes and stress defense: A structure-function update. *J. Plant Physiol.* **2015**, *179*, 40–55. [[CrossRef](#)] [[PubMed](#)]
40. Kavanagh, K.L.; Klimacek, M.; Nidetzky, B.; Wilson, D.K. The structure of apo and holo forms of xylose reductase, a dimeric aldo-keto reductase from *Candida tenuis*. *Biochemistry* **2002**, *41*, 8785–8795. [[CrossRef](#)]
41. De Giuseppe, P.O.; Dos Santos, M.L.; de Sousa, S.M.; Koch, K.E.; Yunes, J.A.; Aparicio, R.; Murakami, M.T. A comparative structural analysis reveals distinctive features of co-factor binding and substrate specificity in plant aldo-keto reductases. *Biochem. Biophys. Res. Commun.* **2016**, *474*, 696–701. [[CrossRef](#)]
42. McElroy, J.S.; Hall, N.D. *Echinochloa colona* with reported resistance to glyphosate conferred by aldo-keto reductase also contains a Pro-106-Thr EPSPS target site mutation. *Plant Physiol.* **2020**, *183*, 447–450. [[CrossRef](#)]
43. Liang, C.; Sun, B.; Meng, Z.; Meng, Z.; Wang, Y.; Sun, G.; Zhu, T.; Lu, W.; Zhang, W.; Malik, W. Co-expression of GR79 EPSPS and GAT yields herbicide-resistant cotton with low glyphosate residues. *Plant Biotechnol. J.* **2017**, *15*, 1622–1629. [[CrossRef](#)]
44. Fartyal, D.; Agarwal, A.; James, D.; Borphukan, B.; Ram, B.; Sheri, V.; Yadav, R.; Manna, M.; Varakumar, P.; Achary, V.M.M. Co-expression of P173S mutant rice EPSPS and *igrA* genes results in higher glyphosate tolerance in transgenic rice. *Front. Plant Sci.* **2018**, *9*, 144. [[CrossRef](#)]
45. Jumper, J.; Evans, R.; Pritzel, A.; Green, T.; Figurnov, M.; Ronneberger, O.; Tunyasuvunakool, K.; Bates, R.; Židek, A.; Potapenko, A.; et al. Highly accurate protein structure prediction with AlphaFold. *Nature* **2021**, *596*, 583–589. [[CrossRef](#)]
46. Varadi, M.; Anyango, S.; Deshpande, M.; Nair, S.; Natassia, C.; Yordanova, G.; Yuan, D.; Stroe, O.; Wood, G.; Laydon, A. AlphaFold Protein Structure Database: Massively expanding the structural coverage of protein-sequence space with high-accuracy models. *Nucleic Acids Res.* **2022**, *50*, D439–D444. [[CrossRef](#)]
47. Xiao, Y.; Zhang, H.; Li, Z.; Huang, T.; Akihiro, T.; Xu, J.; Xu, H.; Lin, F. An amino acid transporter-like protein (OsATL15) facilitates the systematic distribution of thiamethoxam in rice for controlling the brown planthopper. *Plant Biotechnol. J.* **2022**, *20*, 1888–1901. [[CrossRef](#)]

Disclaimer/Publisher’s Note: The statements, opinions and data contained in all publications are solely those of the individual author(s) and contributor(s) and not of MDPI and/or the editor(s). MDPI and/or the editor(s) disclaim responsibility for any injury to people or property resulting from any ideas, methods, instructions or products referred to in the content.